has been established by X-ray diffraction methods in conjunction with chemical analyses and without recourse to MAS NMR methods.

If one could synthesize an SiO_2 modification with the structure of SAPO-31 (instead of just doping $AlPO_4$-31 with silicon) there would be no reason for it to crystallize in the same space group as $AlPO_4$-31 and SAPO-31, namely in $R\bar{3}$ since there is no need to distinguish between Al and P. Thus, the symmetry of the compound could be higher and the space group could be $R\bar{3}m$, a supergroup of $R\bar{3}$. We simulated its crystal structure by distance least squares (using *RERIET*, Kassner, 1993) assuming an Si—O distance of 1.60 Å. In this higher symmetry all O atoms would be located on special positions (site symmetry either 2 or *m*), but none of the Si—O—Si angles would of necessity be straight, thus the simulated structure given here (Table 2) is a likely candidate for a SiO_2 modification with the same topology as $AlPO_4$-31.

Concluding remarks

While the single-crystal structure refinement of SAPO-31 is much more precise than the synchrotron X-ray powder diffraction study of Bennett & Kirchner (1992), it still did not prove possible to locate precisely the template molecules in the pores of SAPO-31, because they are highly disordered. The higher precision makes it possible, however, to find that the Si atoms replace partly the P atoms and not the Al atoms in this microporous molecular sieve.

We thank the Bundesministerium für Forschung und Technologie, the Deutsche Forschungsgemeinschaft, the Polish Committee for Scientific Research (KBN) for support and Reinhard X. Fischer for discussions.

References

BAUR, W. H. (1981). *Structure and Bonding in Crystals*, edited by M. O'KEEFFE & A. NAVROTSKY, Vol. 2, pp. 31–52. New York: Academic Press.
BAUR, W. H. & KASSNER, D. (1991). *Z. Kristallogr.* Suppl. Issue 3, p. 15.
BENNETT, J. M. & KIRCHNER, R. M. (1992). *Zeolites*, **12**, 338–342.
DAVENPORT, G., HALL, S. R. & DREISSIG, W. (1990). *ORTEP*. In *Xtal*3.0 *Reference Manual*, edited by S. R. HALL & J. M. STEWART. Perth: Lamb.
DOWTY, E. (1993). *ATOMS*. Version 2.3. Shape Software, Kingsport, TN.
FINGER, G. & KORNATOWSKI, J. (1990). *Zeolites*, **10**, 615–617.
KASSNER, D. (1993). *RERIET. A Program for Restrained Refinement of Powder Diffraction Data*. Univ. of Frankfurt, Germany.
KASSNER, D., BAUR, W. H., JOSWIG, W., EICHHORN, K., WENDSCHUH-JOSTIES, M. & KUPČIK, V. (1993). *Acta Cryst.* B**49**, 646–654.
KORNATOWKSI, J. & FINGER, G. (1990). *Bull. Soc. Chim. Belg.* **99**, 857–859.
KORNATOWSKI, J., FINGER, G., BAUR, W. H. & ROZWADOWSKI, M. (1993). Polish Patent Appl. 299.039.
LIEBAU, F. (1984). *Acta Cryst.* A**40**, C-254.
MARTENS, J. A., JANSSENS, C., GROBET, P. J., BEYER, H. K. & JACOBS, P. A. (1989). *Zeolites: Facts, Figures, Future*, edited by P. A. JACOBS & R. A. VAN SANTEN, pp. 215–225. Amsterdam: Elsevier.
MEIER, W. M. & OLSON, D. H. (1992). *Atlas of Zeolite Structure Types*, 3rd ed. London: Butterworth.
NGO THONG & SCHWARZENBACH, D. (1979). *Acta Cryst.* A**35**, 658–664.
OLTHOF-HAZEKAMP, R. (1990). *CRYLSQ*. In *Xtal*3.0 *Reference Manual*, edited by S. R. HALL & J. M. STEWART. Perth: Lamb.
STUCKENSCHMIDT, E., JOSWIG, W. & BAUR, W. H. (1993). *Phys. Chem. Miner.* **19**, 562–570.
ZIBROWIUS, B., LÖFFLER, E., FINGER, G., SONNTAG, E., HUNGER, M. & KORNATOWSKI, J. (1991). *Catalysis and Absorption by Zeolites*, edited by G. ÖHLMANN, H. PFEIFFER & R. FRICKE, pp. 537–548. Amsterdam: Elsevier.

Acta Cryst. (1994). B**50**, 294–306

Structure Refinement of the Icosahedral Quasicrystal $Al_{57}Li_{32}Cu_{11}$

BY L. ELCORO AND J. M. PEREZ-MATO

Departamento de Física de la Materia Condensada, Facultad de Ciencias, Universidad del País Vasco, Apdo. 644, *Bilbao, Spain*

(*Received* 24 *July* 1993; *accepted* 16 *November* 1993)

Abstract

The structure of the icosahedral quasicrystal $Al_{57}Li_{32}Cu_{11}$ has been refined within the superspace formalism using symmetry-adapted surface harmonics for the description of the boundaries of atomic surfaces (occupation domains) in internal space. The refinement process has been performed with a general program, *QUASI*, recently developed for this purpose. Besides published neutron and X-ray diffraction data [de Boissieu, Janot, Dubois, Audier & Dubost (1991). *J. Phys. Condens. Matter*, **3**, 1–25],

experimental density and chemical composition were used as control parameters of the fitting. The atomic surfaces were assumed to be parallel to the internal space. No additional *a priori* assumption was introduced, except the limitation on the number of harmonics for describing the contours of the atomic surfaces. The refinement significantly improved previous analyses: starting with a sphere model of the atomic surfaces based on the results of de Boissieu *et al.*, the fit attained R_F (wR_F) values of 0.067 (0.072) and 0.068 (0.068) for X-ray reflections and neutron data, respectively. The final model also rather satisfactorily explains the alternative X-ray data set of Van Smaalen, de Boer and Shen [*Phys. Rev. B* (1991), **43**, 929–937], not included as data in the fitting process. Two and three harmonics are enough to describe the vertex and edge Al/Cu surfaces, respectively, and their shapes approximately coincide with those suggested by de Boissieu *et al.* However, some significant different chemical ordering of the two surfaces can be ascertained. On the other hand, the lithium surface is quite complex and its description requires, at least, four harmonics. Given the scarce number of data, this surface cannot be determined with much accuracy. The presence of nonphysical short interatomic distances in the final structural model is analysed quantitatively.

1. Introduction

Methods for the determination of the structure of quasicrystals (QC) have been greatly improved with the introduction of superspace formalism (Bak, 1985; Janssen, 1986, 1988). Under this approach, structural quantitative analyses of diffraction data have been performed for icosahedral QC (Cahn, Gratias & Mozer, 1988*a*,*b*; Janot, de Boissieu, Dubois & Pannetier, 1989; de Boissieu, Janot & Dubois, 1990; Van Smaalen, 1989; Cornier-Quiquandon, Gratias & Katz, 1991) and decagonal QC (Steurer & Kuo, 1990; Yamamoto, Kato, Shibuya & Takeuchi, 1990; Steurer, 1991). In the case of icosahedral QC, single-crystal diffraction data sets have been obtained for $Al_{57}Li_{32}Cu_{11}$ (de Boissieu, Janot, Dubois, Audier & Dubost, 1991; Elswijk, de Hosson, Van Smaalen & de Boer, 1988; Van Smaalen, de Boer & Shen, 1991), $Al_{62}Cu_{25}Fe_{11}$ (Cornier-Quiquandon *et al.*, 1991) and $Al_{69}Pd_{22}Mn_9$ (Boudard *et al.*, 1992). The structural models resulting from the analysis of these data have not attained accuracies comparable to those common in ordinary structural crystallography. Typically, spherical (shell) models for a few symmetry-independent atomic 'occupation domains' or 'atomic surfaces' (AS) (describing the atomic positions in the superspace formalism) are enough to obtain R factors of the order 0.1–0.2 (Cahn, Gratias & Mozer, 1988*a*; Boudard *et al.*, 1992). However, further quantitative improvement of the model is rather difficult. The case of icosahedral AlLiCu is a clear example of this problem: up to now, three different quantitative models have been proposed. Van Smaalen, de Boer & Shen (1991) could fit, using a decorated three-dimensional Penrose tiling, 37 strong reflections down to wR_{F^2} values of the order 0.05, but 60 additional weaker reflections remained unexplained. de Boissieu, Janot, Dubois, Audier & Dubost (1991) obtained new single-crystal neutron and X-ray diffraction data. Using isotopic substitution, they developed a tentative model, which could be refined down to R_F (wR_F) values of 0.089 (0.090) and 0.078 (0.076) for X-ray (56 reflections) and neutron data (40 reflections), respectively. Finally, Yamamoto (1992), assuming a close similarity of this icosahedral phase with the cubic phase *R*-AlLiCu, proposed an alternative structure, which essentially differs from the previous model by the introduction of an additional low-symmetry AS, while all AS are complex polyhedra described in terms of tetrahedral units; using the same diffraction data as de Boissieu, Janot, Dubois, Audier & Dubost (1991), the model could be refined down to the R values 0.076 and 0.085 for X-ray and neutron data, respectively. Although the last two models mentioned above differ quite significantly (not only in the shape of the AS, but also on their number and positions in the superspace unit cell), the R factors of the two fittings (of the same data) are quite similar.

As an alternative approach to the problem of quantitative structure determination of QC, we previously proposed (Elcoro, Perez-Mato & Madariaga, 1993) a continuous parametrization of the AS contours (under the assumption that the AS are perpendicular to *parallel* space) using truncated series of symmetry-adapted surface harmonics (Bradley & Cracknell, 1972). A general refinement program for polygonal and icosahedral QC, *QUASI*, based on this approach has been developed (Elcoro, Perez-Mato & Madariaga, 1994). In this paper, we present the results obtained for the structure of icosahedral AlLiCu using this program. The resulting structural model yields agreement factors with available diffraction data that are significantly better than any other previously published. The general features of the structure proposed by de Boissieu, Janot, Dubois, Audier & Dubost (1991) are essentially confirmed, except for a significant variation in the degree of chemical disorder of the two Al–Cu AS. On the other hand, the AS describing the lithium positions present a rather complex shape. Some features of the final model seem to support the hypothesis of an additional AS in a low symmetry position, as proposed by Yamamoto (1992). The present work is the first example of the capabilities of using surface

harmonics for the description of AS in QC structures and their refinement.

The paper is organized as follows: in §2, the superspace description of the QC structure, the continuous parametrization of the AS and the structure-factor formulae employed are explained. §3 is devoted to the description of the refinement process and the presentation of its results. Finally, in §4, the main features of the structure are discussed and compared with previous models.

2. Description of the icosahedral structure

We describe the QC structure of $Al_{57}Li_{32}Cu_{11}$ within the superspace formalism (Bak, 1985; Janssen, 1986, 1988) in the form explained by Elcoro, Perez-Mato & Madariaga (1994).

The following wavevectors have been chosen for indexing the diffraction reflections

$$\mathbf{k}_1 = (1/2^{1/2})\,(0,\ 0,\ 1)$$
$$\mathbf{k}_i = (1/2^{1/2})[(2/5^{1/2})\cos(2\pi i/5),$$
$$\times (2/5^{1/2})\sin(2\pi i/5),\ 1/5^{1/2}] \quad i = 2,...,6, \quad (1)$$

where the Cartesian components refer to an orthogonal vector set $\{\mathbf{a}_i^*\}$ with $\mathbf{a}_3^*$ and $\mathbf{a}_2^*$ directed in the diffraction diagram along one of the fivefold axes and a twofold symmetry axis, respectively. According to de Boissieu, Janot, Dubois, Audier & Dubost (1991), $|\mathbf{k}_i| = 0.0989$ Å^{-1} and, therefore, the modulus of the chosen vectors $\mathbf{a}_i^*$ is $|\mathbf{a}_i^*| = 0.1399$ Å^{-1}. Note that this indexation differs from that used in the structure-factor list in de Boissieu, Janot, Dubois, Audier & Dubost (1991) by a simple permutation of the vector indices.

For such a choice of indexing wavevectors, the matrix **A** transforming between the superspace basis associated with the six phases (φ_i) of the structural modulations with wavevectors $\mathbf{k}_i$ and the basis that divides the six-dimensional superspace in the so-called 'parallel' and 'internal' subspaces is chosen as

$$\mathbf{A} = (1/10^{1/2}) \times \begin{bmatrix} 0 & 0 & 2\tau-1 & 0 & 0 & 2\tau-1 \\ -\tau & (\tau-1)(2+\tau)^{1/2} & 1 & -(\tau-1) & (2+\tau)^{1/2} & -1 \\ -\tau & -(\tau-1)(2+\tau)^{1/2} & 1 & -(\tau-1) & -(2+\tau)^{1/2} & -1 \\ \tau-1 & -(2+\tau)^{1/2} & 1 & \tau & (\tau-1)(2+\tau)^{1/2} & -1 \\ 2 & 0 & 1 & -2 & 0 & -1 \\ \tau-1 & (2+\tau)^{1/2} & 1 & \tau & -(\tau-1)(2+\tau)^{1/2} & -1 \end{bmatrix},$$

where $\tau = (5^{1/2}+1)/2$. The relation between both coordinate systems is given by

$$x_i = A_{ji}\varphi_j, \quad (2)$$

where we have taken into account the orthogonality of the chosen matrix **A**. The first three coordinates $\mathbf{x} = (x_1, x_2, x_3)$ correspond to the so-called 'parallel' subspace. This subspace maps real space, with the variables (x_1, x_2, x_3) taken as relative coordinates with respect to the vector set $\{\mathbf{a}_i\}$ defined as the reciprocal set of vectors $\{\mathbf{a}_i^*\}$ used in (1) ($|\mathbf{a}_i| = 1/|\mathbf{a}_i^*| = 7.15$ Å). The last three coordinates in (2), $\mathbf{x}_I = (x_4, x_5, x_6)$ represent the component of the superspace vector in the so-called 'internal' space. Note that superspace coordinates, both φ_i and x_i, are taken adimensional.

From the symmetry properties of the diffraction diagram and the lack of systematic extinctions, the centrosymmetric superspace group $P\bar{5}\bar{3}m$ can be assumed for the QC structure (de Boissieu, Janot, Dubois, Audier & Dubost, 1991). Apart from the translational lattice, this group is generated by the operations $\{S_{51}|000000\}$ and $\{C_{31}|000000\}$ (Janssen, 1988). Their rotational parts in the φ-coordinate system are

$$S_{51} = \begin{pmatrix} -1 & 0 & 0 & 0 & 0 & 0 \\ 0 & 0 & -1 & 0 & 0 & 0 \\ 0 & 0 & 0 & -1 & 0 & 0 \\ 0 & 0 & 0 & 0 & -1 & 0 \\ 0 & 0 & 0 & 0 & 0 & -1 \\ 0 & -1 & 0 & 0 & 0 & 0 \end{pmatrix}$$

$$C_{31} = \begin{pmatrix} 0 & 0 & 0 & 0 & 0 & 1 \\ 1 & 0 & 0 & 0 & 0 & 0 \\ 0 & 0 & 0 & 0 & 1 & 0 \\ 0 & 0 & -1 & 0 & 0 & 0 \\ 0 & 0 & 0 & -1 & 0 & 0 \\ 0 & 1 & 0 & 0 & 0 & 0 \end{pmatrix}. \quad (3)$$

According to de Boissieu, Janot, Dubois, Audier & Dubost (1991), the asymmetric unit in the unit cell of the periodic superspace density that defines the QC structure is formed by three atomic surfaces (AS) perpendicular to parallel space. The positions of their centers, site symmetry, multiplicity, atomic composition and approximate size are indicated in Table 1.

Following the method introduced by Elcoro, Perez-Mato & Madariaga (1993, 1994), the radial functions (external and, if existing, internal) that define the boundaries of the AS are described in terms of linear combinations of orthonormalized 'surface harmonics', $Z_l(\theta,\phi)$, invariant for the AS point symmetry

$$r(\theta,\phi) = \sum_l a_l Z_l(\theta,\phi). \quad (4)$$

The functions $Z_l(\theta,\phi)$ are chosen within the sub-

Table 1. *Main features of the independent atomic surfaces in the structural model of* $Al_{57}Li_{32}Cu_{11}$ *proposed by de Boissieu, Janot, Dubois, Audier & Dubost* (1991)

The approximate size of the AS is represented in the sixth column by the external radius of the spheres considered. The next two columns list the amplitudes a_0^{ex} and a_0^{in} of the zeroth surface harmonic (Y_0^0) corresponding to the external and internal (if any) sphere radius. The columns headed by p_{Al}, p_{Cu} and P_{Li} indicate the atomic occupation probabilities in each atomic surface.

Atomic surfaces	Composition	Center	Site symmetry	Multiplicity	Radius	a_0^{ex}	a_0^{in}	p_{Al}	p_{Cu}	p_{Li}
A_{BC}	Li	$(\frac{1}{2},\frac{1}{2},\frac{1}{2},\frac{1}{2},\frac{1}{2},\frac{1}{2})$	$\bar{5}\bar{3}/m$	1	1.12	3.97	-	0	0	1
A_{OR}	Al/Cu	(0,0,0,0,0,0)	$\bar{5}\bar{3}/m$	1	0.95	3.37	1.14	0.72	0.28	0
A_{ME}	Al/Cu	$(\frac{1}{2},0,0,0,0,0)$	$\bar{5}m$	6	0.69	2.45	-	0.88	0.12	0

spaces generated by the spherical harmonics $Y_l^m(\theta,\phi)$ with a fixed index l

$$Z_l(\theta,\phi) = \sum_{m=-l}^{l} z_{lm} Y_l^m(\theta,\phi). \tag{5}$$

The surface harmonics, $Z_l(\theta,\phi)$, invariant for the site symmetries that are relevant in the present case ($\bar{5}\bar{3}m$ and $\bar{5}m$), are listed by Elcoro, Perez-Mato & Madariaga (1994). Obviously, for any symmetry, the lowest term in (4), Z_o, is the trivial (constant) normalized spherical harmonic $Y_0^0 = 1/(4\pi)^{1/2}$ representing a spherical surface. In general, the linear combination (4) will be typically limited to the lowest order terms. In the present work, the number of terms considered in any of the sums of type (4) is not greater than four. Up to the order considered for every AS, only one invariant harmonic exists (at most) for any index l; this allows the use of l in (4) and (5) as a single label for the invariant harmonic surfaces. For the site symmetry $\bar{5}\bar{3}m$, the first four invariant harmonics correspond to $l = 0$, 6, 10 and 12; their expressions in terms of spherical harmonics are listed by Elcoro, Perez-Mato & Madariaga (1994). For the site symmetry $\bar{5}m$, the lowest three harmonic surfaces are $Y_0^0(\theta,\phi)$, $Y_2^0(\theta,\phi)$ and $Y_4^0(\theta,\phi)$.

We associate a single thermal tensor $\mathbf{B}_\mu$ to all atoms represented by the same AS μ and neglect possible variations within each AS. The site symmetry of the AS also restricts the form of this tensor: For the surfaces of $\bar{5}\bar{3}m$ symmetry, A_{BC} and A_{OR} (see Table 1 for the notation of the AS), the tensor is isotropic ($B_{11} = B_{22} = B_{33} = B$; $B_{ij} = 0$, $i \neq j$), while for A_{ME} of $\bar{5}m$ symmetry (see Table 1), $B_{11} = B_{22} \neq B_{33}$; $B_{ij} = 0$, $i \neq j$.

The expression used for the structure factor is

$$\begin{aligned} F(\mathbf{H}) = [1/V(\mathbf{a}_i)] & \sum_{\mu,m} p_m(\mu) f_m(|\mathbf{H}|) \\ & \times \sum_R \exp[-\tfrac{1}{4}\widetilde{\mathbf{RH}}\mathbf{B}_\mu\mathbf{RH}] \exp[2\pi i \hat{\mathbf{h}}(\hat{\mathbf{R}}\hat{\varphi}_\mu + \hat{\mathbf{t}})] \\ & \times \int_0^\pi \mathrm{d}\theta \sin\theta \\ & \times \int_0^{2\pi} \mathrm{d}\phi \int \frac{\sum_l a_l^{\mu,ex} Z_l(\theta,\phi)}{\sum_l a_l^{\mu,in} Z_l(\theta,\phi)} \mathrm{d}r r^2 \exp(2\pi i \tilde{\mathbf{R}}_l \mathbf{h}_l . \mathbf{x}_l), \end{aligned} \tag{6}$$

where we have taken into account that $|\mathbf{A}| = 1$, and the orientation of the chosen independent AS is a standard one, *i.e.* $\Gamma_\mu = \mathbf{1}$ in the general expression given by Elcoro, Perez-Mato & Madariaga (1994). $V(\mathbf{a}_i)$ is the volume in real space of the cell defined by the vector set $\{\mathbf{a}_i\}$; $p_m(\mu)$ is the occupation probability of the atom species m, with the atomic scattering factor (or scattering length) f_m, in AS μ; $\mathbf{H}$ is the real space diffraction vector, while $\mathbf{h}$ represents the corresponding vector in superspace with integer indices (in the basis $\{\mathbf{k}_i\}$); $\mathbf{h}_I$ is the component of $\mathbf{h}$ in the internal subspace. φ_μ indicates the vector position in superspace of the center of AS μ. The variables (r, θ, ϕ) are spherical coordinates of a generic point $\mathbf{x}_I$ in internal space. The sum in μ extends to the three AS in the asymmetric unit, while m labels the three possible atomic species. The sum in $\{\mathbf{R}|\mathbf{t}\}$ is restricted to a minimal set of operations capable of generating the orbit of symmetry-related AS within the superspace unit cell. $\mathbf{R}$ and $\mathbf{R}_I$ are, respectively, the matrices in parallel and internal space associated to the action of the superspace operation $\hat{\mathbf{R}}$ by the equation

$$\mathbf{A}^{-1}\hat{\mathbf{R}}\mathbf{A} = \begin{pmatrix} \mathbf{R} & 0 \\ 0 & \mathbf{R}_I \end{pmatrix}. \tag{7}$$

According to de Boissieu, Janot, Dubois, Audier & Dubost (1991), the AS are compact except for A_{OR}, which presents a void around its center (see Table 1). Hence, only for this latter AS have we considered a nonzero internal radial function. Initially, only isotropic thermal factors were considered for the three AS. Therefore, apart from the scaling factors of the data sets, the structural parameters to be refined were initially the occupation distribution of aluminium and copper in A_{OR} and A_{ME} [$p_{Al}(A_{OR})$ and $p_{Al}(A_{ME})$], the parameters $a_l^{\mu,ex}$ that define the external contours of the three AS, the parameter $a_l^{OR,in}$ defining the internal boundary of A_{OR} and the three isotropic thermal parameters B_μ.

The relative composition c^m ($\sum c^m = 1$) of a chemical species m is related with these parameters by the expression (Cahn, Gratias & Mozer, 1988*a*)

$$c^m = \sum_\mu p_m(\mu) V_\mu n_\mu / \sum n_\mu V_\mu, \tag{8}$$

where n_μ is the multiplicity in the unit cell of each symmetry-independent AS μ, and V_μ represents the volume in internal space of the corresponding AS

$$V_\mu = \int_0^\pi d\theta \sin\theta \int_0^{2\pi} d\phi \int \frac{\sum_l a_l^{\mu,ex} Z_l(\theta,\phi)}{\sum_l a_l^{\mu,in} Z_l(\theta,\phi)} dr\, r^2. \quad (9)$$

The mass density is also a function of the AS volumes

$$\rho = [1/N_A V(\mathbf{a}_i)] \sum_\mu \sum_m M_m p_m(\mu) V_\mu n_\mu, \quad (10)$$

where M_m is the atomic mass of atom m and N_A is Avogadro's number.

In order to illustrate from a practical viewpoint how the structural parameters introduced above define the real space QC structure, it is interesting to describe briefly a numerical method for determining, from the structural parameters above, the actual atomic positions in real space: Starting from the centers of the AS in the asymmetric unit and using the six-dimensional superspace group rotational and translational operations, the positions $\{\varphi_\mu\}$ in superspace that represent the centers of all the AS within some adequate close domain of superspace unit cells are calculated. By means of (2), the parallel and internal components $\mathbf{x}_\nu$ and $\mathbf{x}_{I\nu}$ of each AS center φ_ν are determined. Every AS ν that intersects the plane $\mathbf{x}_I = 0$ locates an atom (of the type associated to the AS) in real space at the position given by the coordinates $\mathbf{x}_\nu$ (relative to the vector basis $\{\mathbf{a}_i\}$). Therefore, the problem reduces to determine for every AS ν, whether the point $(\mathbf{x}_\nu,0)$ belongs to the AS or not. This can be done in the following way: the vector $(-\mathbf{x}_{I\nu})$ in internal space is expressed in spherical coordinates with respect to the pertinent coordinate system $(r_\nu, \theta_\nu, \phi_\nu)$. Then, the AS intersects the plane $\mathbf{x}_I = 0$ if the value of r_ν is intermediate between the values of the two radial functions r^{in} and r^{ex}, which describe the contours of the AS for the orientation $(\theta_\nu, \varphi_\nu)$: $r_\nu^{in}(\theta_\nu, \phi_\nu) \le r_\nu \le r_\nu^{ex}(\theta_\nu, \phi_\nu)$. If AS ν is obtained by means of a symmetry operation $\{\mathbf{R}|\mathbf{t}\}$ from an AS μ in the asymmetric unit, we can express the previous condition in terms of radial functions of the AS in the asymmetric unit $r_\mu^{in}(\theta'_\nu, \phi'_\nu) \le r_\nu \le r_\mu^{ex}(\theta'_\nu, \phi'_\nu)$, where (θ'_ν, ϕ'_ν) represents the orientation of the vector $R_I^{-1}(-\mathbf{x}_{I\nu})$.

3. Refinement process

The two data sets published by de Boissieu, Janot, Dubois, Audier & Dubost (1991) were used as experimental single-crystal diffraction data: 56 X-ray reflections with Mo radiation ($\lambda = 0.7107$ Å) and a neutron diffraction data set of 40 reflections for neutrons with $\lambda = 1.26$ Å. All reflections satisfy $I > 3\sigma$ and were considered observed in the refinement. The maximum $\sin\theta/\lambda$ are 0.5111 and 0.7129 $Å^{-1}$ for the X-ray and neutron data, respectively. No absorption or extinction corrections were attempted. Experimental values of the mass density and precise chemical composition of the samples used for the diffraction experiments were also reported in the same reference

$$\begin{aligned} \rho_o &= 2.47 \pm 0.01 \text{ g cm}^{-3} \\ c_o^{Al} &= 0.57 \pm 0.02 \\ c_o^{Cu} &= 0.11 \pm 0.01 \\ c_o^{Li} &= 0.32 \pm 0.01. \end{aligned} \quad (11)$$

The X-ray data reported by Van Smaalen, de Boer & Shen (1991), consisting of 96 reflections for Mo radiation ($\lambda = 0.7107$ Å) with $I > 2\sigma$, was not considered in the refinement but was used *a posteriori* as an additional check of the reliability of the structural model. For the refinement, the program *QUASI* (Elcoro, Perez-Mato & Madariaga, 1994) was employed. This program minimizes the quantity, χ^2, defined as

$$\chi^2 = \frac{\sum_{\mathbf{H}} w_{\mathbf{H}}(F_o(\mathbf{H}) - k|F_c(\mathbf{H})|)^2}{\sum_{\mathbf{H}} w_{\mathbf{H}} F_o^2(\mathbf{H})} + w_c \frac{\sum_m (c_o^m - c_c^m)^2}{\sum_m (c_o^m)^2} + w_\rho \frac{(\rho_o - \rho_c)^2}{\rho_o^2}, \quad (12)$$

with the scale factor k included among the adjusted parameters. ρ_o, ρ_c, c_o^m and c_c^m are the experimental and calculated mass densities and relative atomic compositions, respectively. The strengths of the restraints with respect to mass density and atomic composition were controlled by the weight parameters w_ρ and w_c, so that the structural model always kept reasonable values for these parameters. The first term in (12) represents the square of the weighted agreement factor for the structure-factor moduli, wR_F. When the two data sets were simultaneously refined, two terms of this type (one for each set) were included in χ^2. The usual $1/\sigma^2$ was introduced as the weighting scheme. Atomic scattering factors and neutron scattering lengths were taken from *International Tables for X-ray Crystallography* (1974) and Koester (1977), respectively. Anomalous dispersion was included for X-ray factors.

The program *QUASI* allows for performing the minimization process by means of two alternative methods: a full least-squares process or a *SIMPLEX* algorithm (Nelder & Mead, 1965). The number of points for the Gaussian numerical calculation of the integrals in (6) and (9) was set to 20, which, in

Table 2. *Agreement factors of the different data sets for the models obtained in successive refinement steps explained in the text*

In the the case of the X-ray data from Van Smaalen, de Boer & Shen (1991), the first row indicates the agreement factors for the whole data set, while the second corresponds to the subset of 44 reflections with $I > 3\sigma$. Models 1 and 2 refer to preliminary models obtained from fitting only the X-ray data (model 1) or neutron data (model 2) from de Boissieu, Janot, Dubois, Audier & Dubost (1991). For refinements simultaneously using both data, models 4 and 3 are, respectively, the results with and without anisotropic thermal parameters for A_{ME}.

	X-ray data		Neutron data		X-ray data*	
	R	wR	R	wR	R	wR
					0.29	0.13
Model 1	0.065	0.068	0.106	0.104	0.121	0.098
					0.27	0.13
Model 2	0.083	0.088	0.073	0.075	0.106	0.089
					0.28	0.12
Model 3	0.075	0.075	0.076	0.076	0.105	0.088
					0.27	0.12
Model 4	0.067	0.072	0.068	0.068	0.097	0.082

* Van Smaalen, de Boer & Shen (1991).

general, was enough for obtaining three significant digits of the R factors.

As a starting model for the refinement, a sphere model (see Table 1) of the AS based on the results of de Boissieu, Janot, Dubois, Audier & Dubost (1991) was used. The process can be essentially summarized as follows: the sphere model with isotropic thermal parameters was optimized up to wR values of the order 0.24 and 0.15 for X-ray and neutron data, respectively. Successive higher harmonics for the AS external radial functions were included in the refinement. The internal radial function of A_{OR} was, however, always limited to a spherical function. With three harmonics for the external radial functions of all AS, and adjusting the thermal parameters in the final stages, the weighted R factors decreased to 0.09 (X-ray) and 0.08 (neutrons). The third harmonic for A_{OR} was, however, negligible, having a large standard deviation. In a subsequent refinement, the addition of a fourth harmonic in the AS external radial functions caused no significant improvement of the fitting, except in the case of the lithium surface (A_{BC}); for the other two AS, the values of the fourth harmonic showed great standard deviations, their influence in the fitting being rather weak. Consequently, thereafter, the external radial function expressions were limited to 4, 2 and 3 harmonics for A_{BC}, A_{OR} and A_{ME}, respectively. Hence, the maximum number of adjustable structural parameters was 15. At this stage, least-squares processes did not converge properly and several solutions with similar wR factors, of the order 0.08, were obtained. The models were essentially identical except for the lithium surface, which differed greatly in its external contours. On the other hand, in all cases, the chemical composition of the aluminium/copper surfaces, indicated that within the standard deviations A_{OR} was very close to a 1:1 Al–Cu mixture, while A_{ME} was essentially formed by Al atoms.

At this point, the alternative of the simplex algorithm was employed to fit the X-ray and neutron data separately. In Table 2, the final agreement factors of each fit (models 1 and 2) are summarized. As additional information, the R values of each model for the X-ray data set of Van Smaalen, de Boer & Shen (1991), obtained adjusting only a scale factor, are also given. It can be seen that the solution

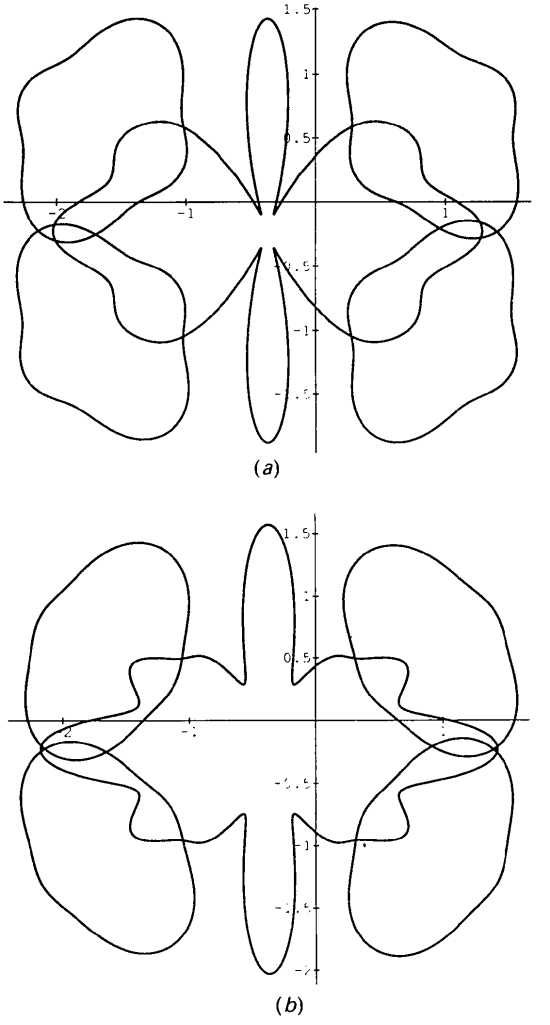

Fig. 1. Section x_4–x_6 in internal space of A_{BC} passing through its center, together with the projection on this plane of four symmetry-related A_{ME} for the refined models using only (*a*) the X-ray data set (model 1 in Table 2) and (*b*) the neutron data set (model 2 in Table 2) of de Boissieu, Janot, Dubois, Audier & Dubost (1991). The section contains two fivefold, two threefold and two twofold axes. The reference axes are depicted along the two twofold axes and do not, therefore, represent the x_4 and x_6 coordinates.

obtained from the fit of only 40 neutron reflections is already enough to explain the X-ray data sets of de Boissieu, Janot, Dubois, Audier & Dubost (1991) and Van Smaalen, de Boer & Shen (1991) up to wR values of the order 0.09 and 0.13, respectively. The most significant differences between the models obtained from X-ray and neutron data are found in the shape of the lithium surface and its thermal parameter.

When the AS are projected on the internal space, a superposition of the lithium surface (A_{BC}) with A_{ME} is present in both models (see Fig. 1). This superposition implies the existence in the structural model of nonphysical interatomic distances of *ca* 0.6 Å between pairs of Li and Al/Cu atoms, represented by the parts of the AS that superpose (de Boissieu, Janot, Dubois, Audier & Dubost, 1991). As could be expected from the scarce sensitivity of X-ray diffraction to Li atoms, the superposition volume between both AS is especially large in the case of the model obtained fitting only X-ray data.

The simplex minimization procedure was then employed to simultaneously fit both neutron and X-ray data, including the two previous models in the starting solutions; the R (wR) values attained were of the order 0.075 for both data sets (see model 3 in Table 2) and the lithium surface acquired a shape which can be considered as a compromise between the two preceding solutions, but closer to the neutron solution (model 2 in Table 2). Finally, the symmetry-allowed anisotropy of the thermal tensor for A_{ME} ($B_{11} = B_{22} \neq B_{33}$) was introduced. The addition of this new parameter, which increased the number of adjustable parameters to 18 (including the two scale parameters), significantly improved the fitting. The R values of this final model (model 4 in Table 2) decreased by almost 1% in the case of neutron data, demonstrating the physical relevance of this new parameter. Final R (wR) values are 0.068 (0.068) for neutron and 0.067 (0.072) for X-ray data with a goodness-of-fit of 3.57.* The calculated atomic composition and mass density for the model are $Al_{56.4}Li_{31.9}Cu_{11.7}$ and 2.467 g cm^{-3}, respectively, which are in excellent agreement with the experimental values [see (11)]. The quality of the final fit is visualized in Fig. 2, where calculated and observed structure factors are compared graphically. In the same figure, a similar comparison is also shown for the data set of Van Smaalen, de Boer & Shen (1991). It can be seen that the agreement of this additional data is comparable to that obtained for the refined X-ray data set, except for the weaker reflections. These latter reflections systematically have larger values than predicted and increase the global wR factors to 12%. It should be pointed out, however, that this data set includes reflections with $I > 2\sigma$ and for the 44 reflections with $I > 3\sigma$, the wR factor reduces to 0.082.

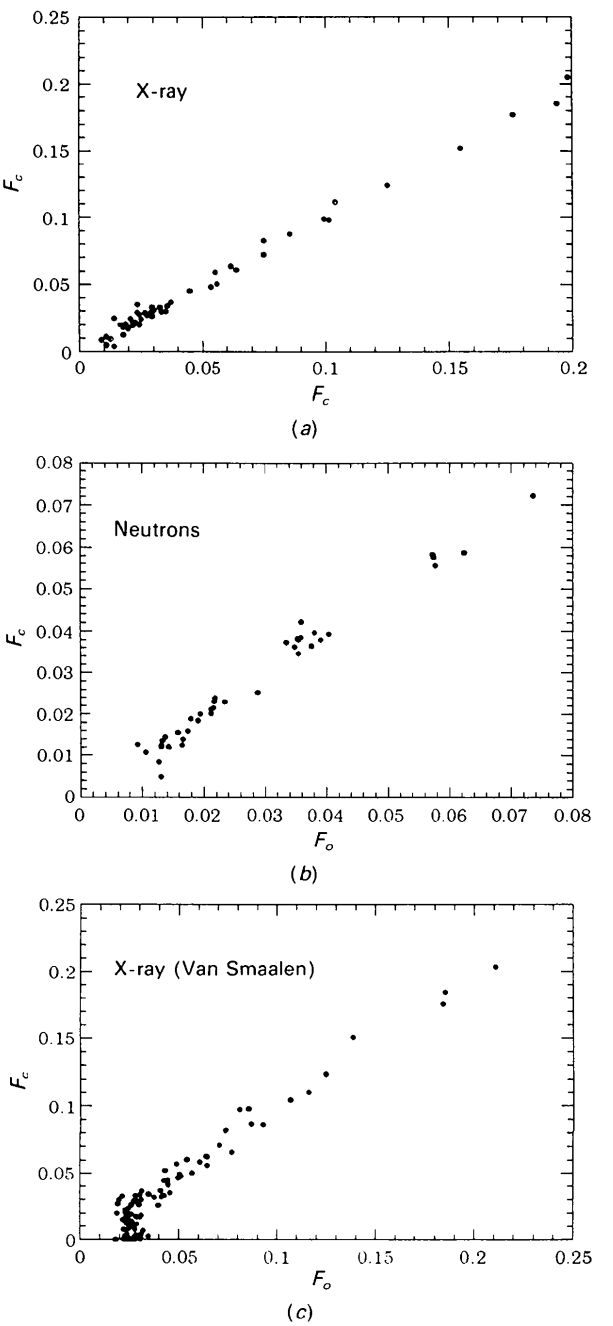

Fig. 2. $F_{cal}(\mathbf{H})$ *versus* $F_{obs}(\mathbf{H})/k$ plots of the final model for (*a*) the X-ray data set of de Boissieu, Janot, Dubois, Audier & Dubost (1991), (*b*) the neutron data set of the same reference and (*c*) the X-ray data set of Van Smaalen, de Boer & Shen (1991).

* A list of structure factors has been deposited with the British Library Document Supply Centre as Supplementary Publication No. SUP 71659 (5 pp.). Copies may be obtained through The Managing Editor, International Union of Crystallography, 5 Abbey Square, Chester CH1 2HU, England.

Table 3. *Structural parameters of quasicrystalline* $Al_{57}Li_{32}Cu_{11}$ *corresponding to model* 4

Thermal parameters are given in Å^2 for the expression $\exp(-\frac{1}{4}\sum B_{ij}H_iH_ja_i^*a_j^*)$ with the components H_i of the diffraction vector on the basis of $\{\mathbf{a}_i^*\}$ indicated in the text. In the case of the first two atomic surfaces, column B indicates the isotropic thermal parameter, while for the third AS it represents the value of $B_{11}(=B_{22})$. Parameters not refined are indicated with an asterisk.

Atomic surfaces	a_1^{ex}	a_2^{ex}	a_3^{ex}	a_4^{ex}	a_1^{in}	B	B_{33}	p_{Al}	p_{Cu}	p_{Li}
A_{BC}	4.00 (1)	−0.53 (1)	−0.63 (3)	0.35 (10)	–	2.76 (6)	–	0*	0*	1*
A_{OR}	3.25 (2)	0.21 (6)	–	–	1.43 (3)	2.31 (8)	–	0.54 (1)	0.46 (1)	0*
A_{ME}	2.70 (1)	−0.37 (5)	0.17 (10)	–	–	1.8 (4)	2.7 (2)	0.899 (6)	0.101 (6)	0*

A section of the projection on the internal space of the A_{BC} and A_{ME} surfaces for this final model is depicted in Fig. 3; it can be seen that the significant improvement of the adjustment when allowance for the anisotropy of the thermal tensor of A_{ME} was introduced can be related to a large variation of the contours of the lithium surface that now are broadly correlated with those of A_{ME}, so that the nonphysical superposition region discussed above is somehow reduced. This correlation between both AS, which appears spontaneously in the refinement, is the best proof that the model is a good approximation to the real structure and confirms the importance of taking into account the symmetry-allowed thermal anisotropy of A_{ME}. The thermal parameter B_{33} of the Al/Cu atoms in A_{ME}, associated to the atomic thermal displacements in real space along a fivefold axis, is significantly larger than those corresponding to the two perpendicular directions (see Table 3). In fact, the interatomic vectors in real space corresponding to atom pairs at nonphysical short distances, resulting from the superposition in internal space of A_{ME} and A_{BC}, are along this fivefold direction. Hence, it seems that when the anisotropy of thermal parameters of A_{ME} is not included, the refinement tends to superpose spuriously both surfaces, so that the presence of lithium at distances of the order of atomic thermal displacements would simulate the effect of a larger thermal parameter. A partial superposition in internal space of both surfaces is still present but is considerably smaller than those refined with isotropic thermal parameters. The volume of the superposed region between the A_{BC} surface and one A_{ME} is 0.19, while the total volume of A_{BC} is 6.952. Taking into account that the number of symmetry-equivalent superposition regions is 12, we then have about 30% of the Li atoms in the wrong positions or, inversely, about 18% of the Al/Cu atoms of the A_{ME} surface.

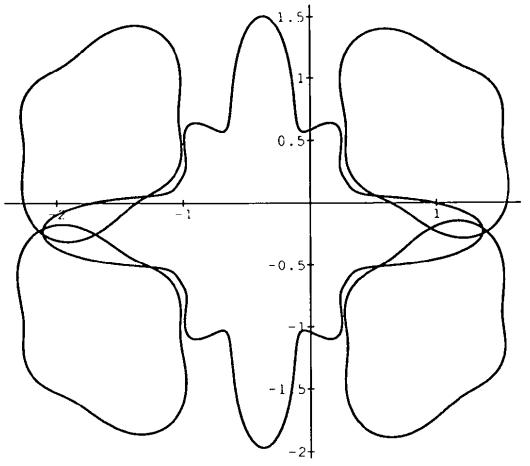

Fig. 3. Same as in Fig. 1 for the final refined model (model 4 in Table 2).

It could be argued (Steurer, 1990) that diffraction analysis only provides information on the average structure and then such superpositions are acceptable if both surfaces are not fully occupied. The superposition would then indicate some disorder, so that the atomic positions resulting from both AS are not occupied simultaneously. However, in the present case, the surfaces have been assumed to be fully occupied and the possibility of this disorder cannot be checked, since the number of adjustable parameters, considering the scarce amount of data, would increase to unreasonable values. In any case, it must be stressed that despite the non-negligible superposition of both surfaces, the surface contours in the final model show a clear tendency to keep unsuperposed, showing in this sense a correlation which was not included *a priori* in the refinement. In any case, the form given to the AS of Li in the final model should be taken with caution, and only as a starting point of any further modelling. Also, a small superposition of symmetry-related A_{ME} can be observed in Fig. 3. This is also a nonphysical feature, as the corresponding atom pairs would be at distances of the order 1 Å. However, the superposition volume is in this case rather small.

Despite these nonphysical features, the quality of the model could be ascertained by means of X-ray difference Fourier maps in internal space. Around A_{OR}, the highest peaks in difference Fourier maps are not greater than 1.5 e Å^{-3}, while in A_{ME} they are lower than 1 e Å^{-3}. In A_{BC}, although the peaks in the difference map are of the same order of magnitude (0.9 e Å^{-3}) as in the other AS (see Fig. 4), the values are in this case of the order 10% of the absolute electron density, indicating an important

uncertainty on the AS form. Although, the model is expected to introduce excess electron density in the superposition regions mentioned above, the map in this region indicates nothing in this sense since $\Delta\rho$ is positive here for a map constructed with $F_o - F_c$. It must be noted that Fourier maps restricted to internal space, with the parallel coordinates fixed to those corresponding to a certain AS, only include the maxima of the atomic electron density on its spreading along the parallel space. Therefore, the difference Fourier maps calculated in this form should contain the highest peaks if these are due to deviations of AS shapes in internal space with respect to those in the real system.

4. Discussion

The structural parameters of the final model (model 4 in Table 2) are listed in Table 3. The dubious character of the details assigned to the contours of A_{BC} are evidenced in the high standard deviation of the amplitude of its fourth harmonic, which is as high as 30%. Also, the third harmonic associated to A_{ME} presents a large error. This means that the nonphysical superposition regions mentioned in the previous section are essentially within the error intervals of the AS contours. In Figs. 5, 6 and 7, the three AS are depicted by means of a three-dimensional scheme and a section in the x_4–x_6 plane (perpendicular to a twofold axis in the internal space). Atomic surfaces A_{OR} and A_{ME} essentially coincide with those proposed by de Boissieu, Janot, Dubois, Audier & Dubost (1991). The amplitudes corresponding to the zeroth harmonic are very close to those of the starting sphere model (*cf.* Tables 1 and 3), except for that of A_{ME} and the interior void of A_{OR}, which have a small significant difference. However, the most rele-

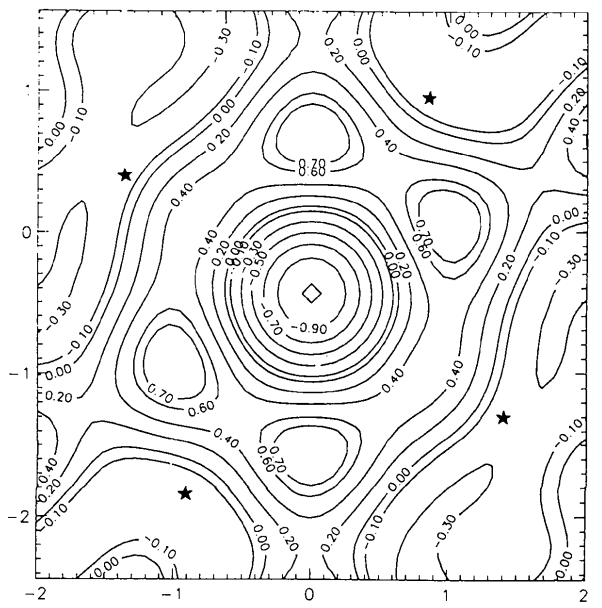

Fig. 4. Difference Fourier map of the central section x_4–x_6 of A_{BC} for the X-ray data set of de Boissieu, Janot, Dubois, Audier & Dubost (1991) and the final model. Horizontal and vertical reference axes correspond to x_4 and x_6, respectively. The x_6 axis is directed along a fivefold axis. Centers of the hypothetical additional Al atomic surfaces proposed by Yamamoto (1992) are indicated with a star.

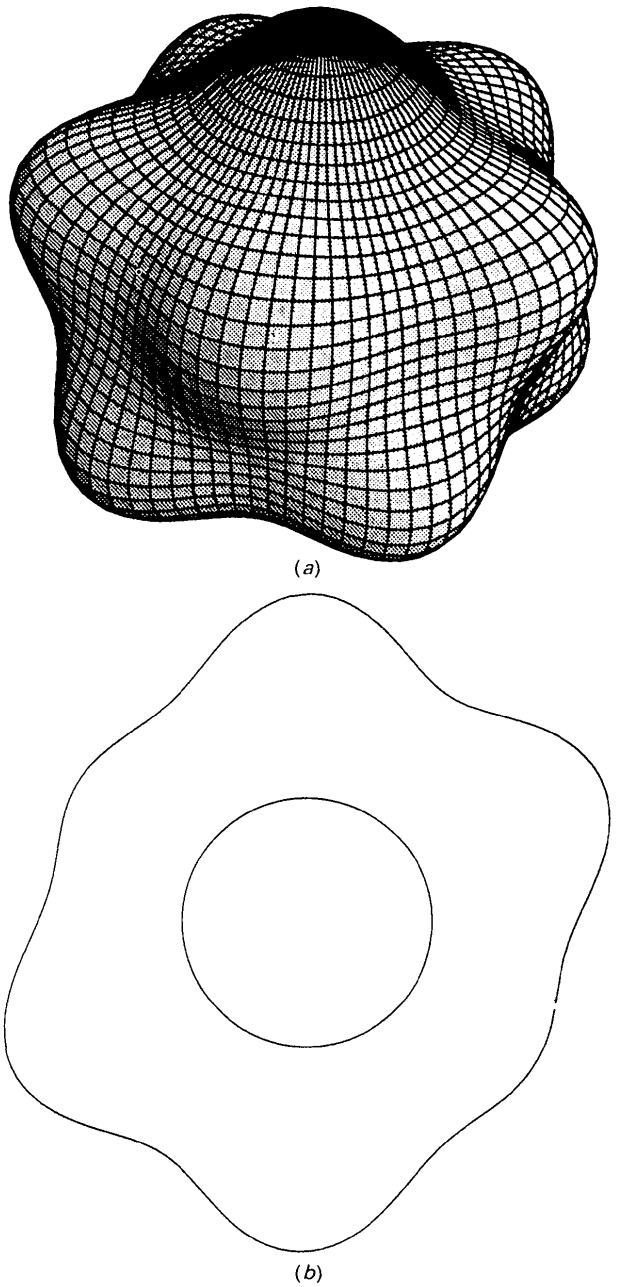

Fig. 5. (*a*) Three-dimensional representation of A_{OR} and (*b*) the central section x_4–x_6 of A_{OR} with x_6 along the vertical direction.

vant difference with respect to the model proposed by de Boissieu, Janot, Dubois, Audier & Dubost (1991) concerns the degree of chemical disorder of both A_{OR} and A_{ME}. In this reference, a disorder close to the total randomness of aluminium and copper was proposed. Taking into account the relative concentration of both atoms, this would correspond to an occupation probability of 0.84 for aluminium in both AS. The present analysis, however, indicates a rather different situation in the two AS. Systematically and from the first steps, the refinement was directed towards an occupation probability of the atomic positions associated to the A_{OR} close to 50/50 distribution, while A_{ME} pointed to an occupation mainly associated with aluminium (90%). Note the small standard deviations obtained for the corresponding occupation probabilities in Table 3, which support the validity of this result.

The thermal parameters for A_{ME} and A_{BC} coincide within standard deviations with those obtained by Yamamoto (1992), but in the present analysis the standard deviations are almost one order of magnitude smaller; in the case of A_{ME}, as the anisotropy of its thermal tensor was not considered before, a direct comparison is not possible. It is important, however, to note that β_{11} coincides with the value obtained by Yamamoto for the isotropic thermal parameter,

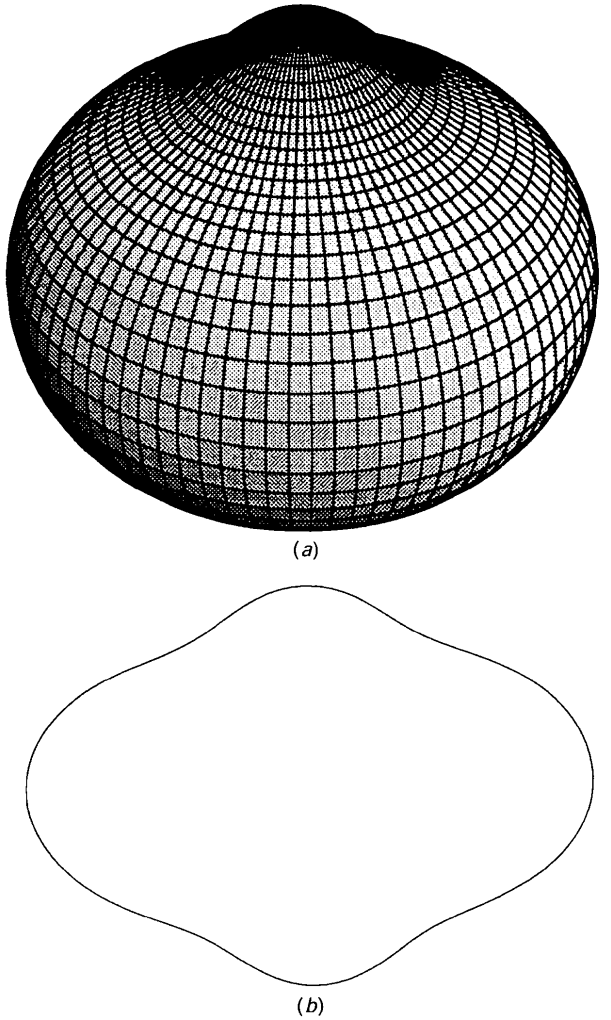

Fig. 6. (*a*) Three-dimensional representation of A_{ME} and (*b*) the central section x_4–x_6 of A_{ME} with x_6 along the vertical direction.

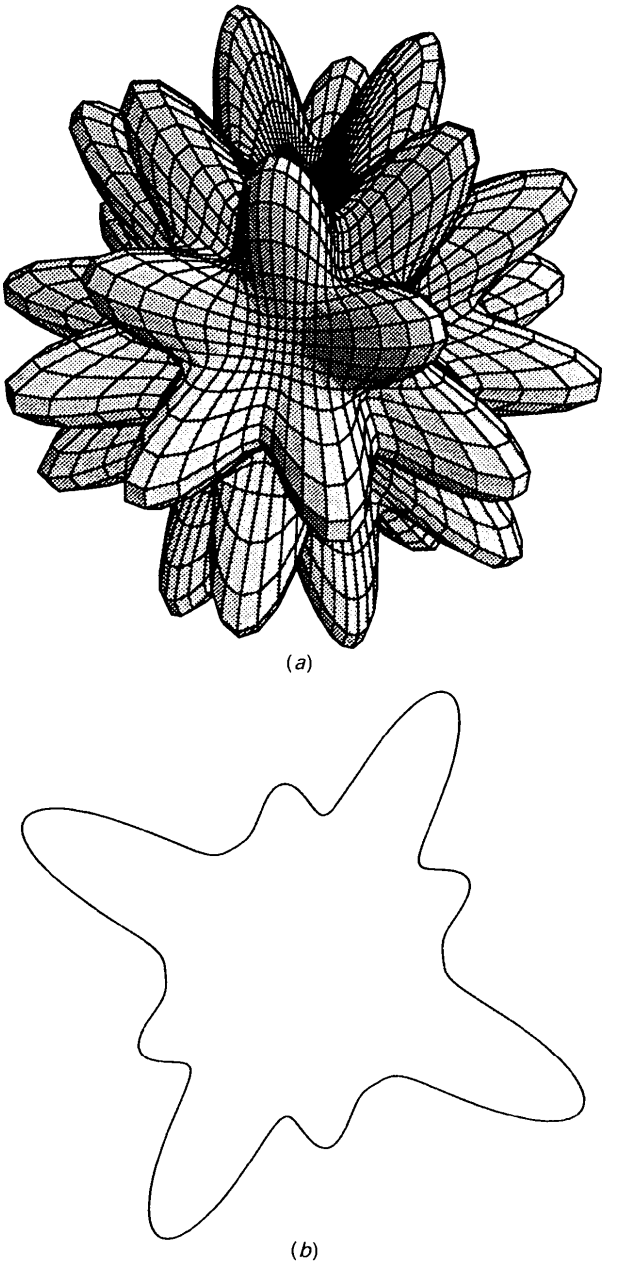

Fig. 7. (*a*) Three-dimensional representation of A_{BC} and (*b*) the central section x_4–x_6 of A_{BC} with x_6 along the vertical direction.

while β_{33}, corresponding to the fivefold direction, is significantly larger (50%).

Although the triacontahedron is often the shape associated to the AS at the origin in some of the previous models of AlLiCu (Van Smaalen, de Boer & Shen 1991; Yamamoto, 1992) and other icosahedral QC (Cornier-Quiquandon *et al.*, 1991), A_{OR} is more of an icosahedron (see Fig. 5). The contours of A_{ME} (Fig. 6) are described approximately by an ellipsoid with its shorter axis along the fivefold direction and the other two forced by symmetry to be equal. On the other hand, the shape of A_{BC} (Fig. 7) is rather complicated and looks quite different from the polyhedra discussed in Cornier-Quiquandon *et al.* (1991) and Yamamoto (1992), as its 'vertices' are directed along the twofold axes.

X-ray Fourier maps such as those shown in Fig. 8, compared with Figs. 5 and 6, confirm the correctness of the shapes associated to A_{OR} and A_{ME}. The void at the center of A_{OR} is only reflected in the map by a small depression of the density at the AS center. The depression is clearly smaller than the hypothesized void; this is a typical truncation effect of the Fourier series, since in the corresponding difference Fourier map the values of $\Delta\rho$ in this region do not exceed 1.5 e $Å^{-3}$. Truncation effects also probably cause the maximum electron densities at A_{ME} and A_{OR} to be comparable, despite the significant difference in chemical composition and hence in the number of electrons per effective atom in the two AS. This is also supported by the small values of $\Delta\rho$ in both AS. It should be stressed that the signs associated with the observed structure factors for calculating the Fourier maps are weakly dependent on the details of the AS shapes. Indeed, eliminating the small phase shifts due to the consideration of anomalous scattering in the present analysis, the signs associated in the present model to the X-ray and neutron reflections coincide without exception with those resulting from the model of de Boissieu, Janot, Dubois, Audier & Dubost (1991), although the shape of A_{BC} in this model significantly differs from that obtained here. The Fourier maps for both neutrons and X-ray are, therefore, essentially independent of the assumed model details. This allows the use of the Fourier map of A_{BC} to elucidate the real significance of the shape obtained in the refinement. Fig. 9 shows a section (x_4–x_6) of the Fourier maps obtained with the X-ray and neutron data. The X-ray map is complicated by the presence of considerable electron density from A_{ME}. As the two surfaces are only about 0.5 Å distant along parallel space, the spread in parallel space of the electron density associated with the Al/Cu atoms of A_{ME} makes it still significant at the position in parallel space corresponding to A_{BC}. In fact, the absolute maxima of the map in Fig. 9(*a*) are centered at the points corresponding to the projection of the centers of A_{ME} (compare with Fig. 3). An elongation along the two perpendicular twofold axes of the electron density corresponding to A_{BC} can be observed, in accordance with the shape in the model (see Fig. 7). The other local maxima and minima can be attributed to truncation effects, due to the complex contours of A_{BC}. A much simpler picture

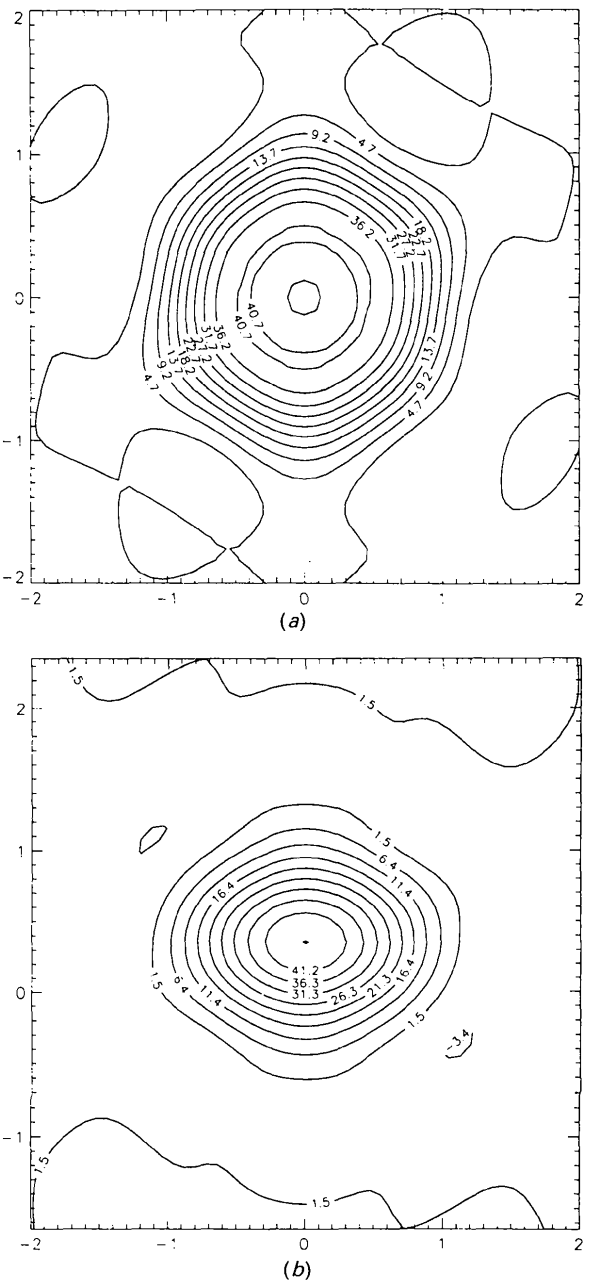

Fig. 8. Fourier maps of the central section x_4–x_6 of (*a*) A_{OR} and (*b*) A_{ME} for the X-ray data set of de Boissieu, Janot, Dubois, Audier & Dubost (1991). Reference axes are orientated in the same way as in Fig. 4.

appears in Fig. 9(*b*), where the problem of the superposition of scattering densities of different AS is not critical. Definitely, the surface is elongated along the two twofold axes, but the map does not reveal the complex contours suggested by the model. On the other hand, the X-ray map has a much richer structure that follows broadly the AS contours given in the model (compare with Fig. 7*b*).

The possible existence of the fourth AS of aluminium proposed by Yamamoto (1992) can be investigated in the previous maps. According to Yamamoto (1992), this additional AS of aluminium would be situated on a twofold axis and its center has the same position in parallel space as A_{BC}. Hence, the section depicted in Figs. 4, 7 and 9 for A_{BC} should also contain the centers of four of these (symmetry equivalent) AS. Their centers in internal space proposed by Yamamoto (1992) would be situated in our representation at (−1.34, 0, 0.39) (0.83, 0, 0.90), (1.34, 0, −1.26) and (−0.83, 0, −1.78). These points are indicated in Figs. 4 and 9 with a star. Indeed, according to Fig. 9(*a*), a significant electron density of the order 6 e Å^{-3} is localized around these points and two of them form clear maxima in the two-dimensional map. It is interesting that the points are approximately on the center of the spurious superposition regions of the A_{BC} and A_{ME} surfaces. So, it looks as if the refinement introduces these non-physical features in the model in order to produce larger electron densities in these regions, in accordance with the presence of a fourth AS with larger atomic number at these points. On the other hand, the electron-density values involved seem rather low to be associated with aluminium. One should have in mind that in general, Li and Al atoms are expected to produce peaks of the order 9 and 50 e Å^{-3}, respectively, in real space electron-density maps obtained in the best conditions. In addition, the $\Delta\rho$ represented in Fig. 4 has values of the order only 0.1 e Å^{-3} in these regions, indicating that the mentioned features of the electron-density map are consistent with the model of only three independent surfaces, and, given the weak dependence of the structure factors on the details of the A_{BC} contours, one can advance that the main features of this $\Delta\rho$ map would not vary much after an adequate 'tailoring' of A_{BC}, which eliminates the spurious superpositions. Also, the neutron map shows no clear evidence of additional AS. A comparison with analogous difference Fourier and Fourier maps of the model proposed by Yamamoto (1992) would be interesting for elucidating this point.

5. Concluding remarks

We have presented the first example of the use of the program *QUASI* for the structural analysis of quasicrystals. The method is based on the use of symmetry-adapted surface harmonics for the description of the contours of the atomic surfaces in internal space. The results look promising. The method leads to a structural model of $Al_{57}Li_{32}Cu_{11}$ with weighted

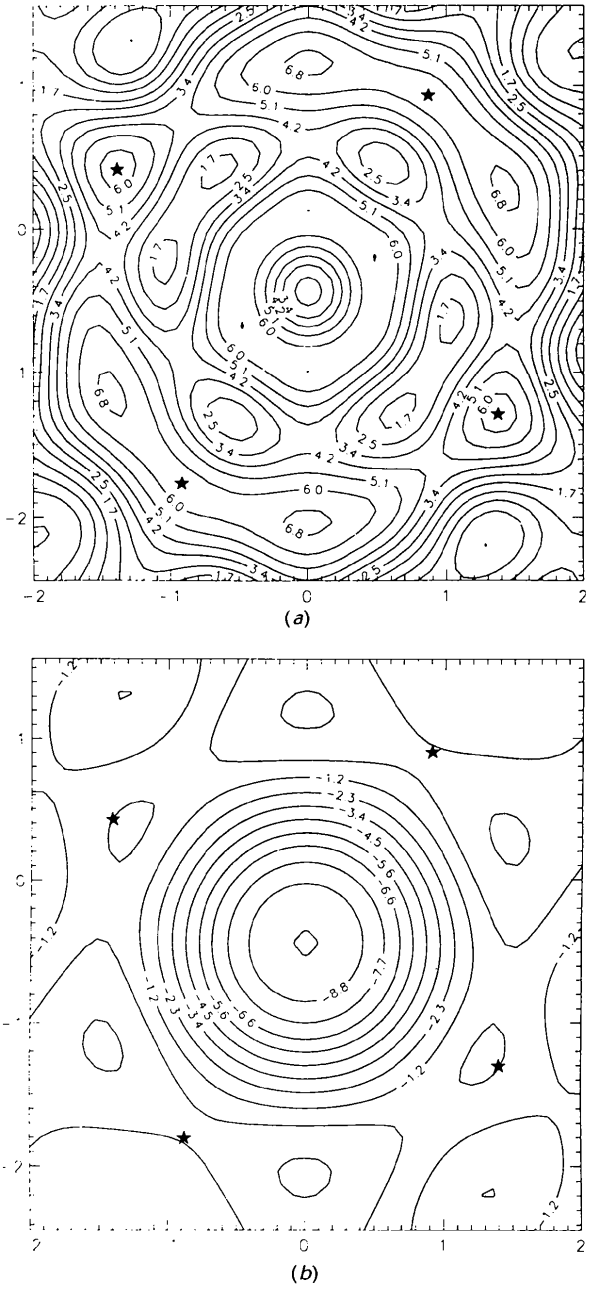

Fig. 9. Fourier maps of the central section x_4–x_6 of A_{BC} for (*a*) the X-ray data set of de Boissieu, Janot, Dubois, Audier & Dubost (1991) and (*b*) the neutron data set of the same work. Reference axes are oriented in the same way as in Fig. 4. Centers of the hypothetical additional Al atomic surfaces proposed by Yamamoto (1992) are indicated with a star.

R factors, which improves previously published models by one or two percentage points. The main features of the model essentially confirm the structure proposed in de Boissieu, Janot, Dubois, Audier & Dubost (1991), except for some significant variation of the detailed shape of the lithium surface and the chemical disorder of the other two. The refinement has been performed with a very low ratio of data *versus* variables (*ca* 5–6), but using mainly a direct minimum search (instead of a least-squares algorithm) restrained by the deviations of the calculated chemical composition and mass density with respect to the observed values. The importance should be stressed of having accurate experimental values of these quantities (with a precise estimation of their errors) for performing a meaningful refinement process. In contrast to standard crystallography, both chemical composition and mass density depend on the model parameters to be adjusted. Therefore, the values resulting from the model should be compared with the experimental values all along the refinement process, taking into account the error margins. For instance, much larger errors than those assumed in the present work for the experimental composition and density of the icosahedral AlLiCu could lead to important variations in the best model, particularly the shape of the lithium surface, which could give equal or better *R* factors, while keeping the model density and chemical composition within the new error margins.

The final structural model includes some nonphysically short interatomic distances. Although in a small ratio, they are, however, enough to preclude an analysis of the model in real space. Previous to such an analysis, slight corrections of the atomic surfaces of the model that avoid these nonphysical features will be necessary. An obvious procedure for this additional step is to include an additional penalty function in the refinement process, penalizing the existence of too short interatomic distances in the model (Elcoro, Perez-Mato & Madariaga, 1994). Such a method, however, has failed until now due to the lack of enough accuracy (compatible with acceptable computer time costs) for the required three-dimensional numerical integration of the superposition regions of atomic surfaces.

We gratefully acknowledge M. de Boissieu and S. Van Smaalen for providing the data sets used and for helpful comments. This work has been partially supported by the UPV (project UPV 063.310-E081/91) and the DGICYT (project PB91-0448). One of us (LE) is indebted to the Basque Government for financial support.

References

Bak, P. (1985) *Phys. Rev. B*, **32**, 5764–5772.
Boissieu, M. de, Janot, C. & Dubois, J. M. (1990). *J. Phys. Condens. Matter*, **2**, 2499–2517.
Boissieu, M. de, Janot, C., Dubois, J. M., Audier, M. & Dubost, J. (1991). *J. Phys. Condens. Matter*, **3**, 1–25.
Boudard, M., Boissieu, M. de, Janot, C., Heger, G., Beeli, C., Nissen, H.-U., Vincent, H., Ibberson, R., Audier, M. & Dubois, J. M. (1992). *J. Phys. Condens. Matter*, **4**, 10149–10168.
Bradley, C. J. & Cracknell, A. P. (1972). *The Mathematical Theory of Symmetry in Solids*. Oxford: Clarendon Press.
Cahn, J. W., Gratias, D. & Mozer, B. (1988*a*). *J. Phys. (Paris)*, **49**, 1225–1233.
Cahn, J. W., Gratias, D. & Mozer, B. (1988*b*). *Phys. Rev. B*, **38**, 1638–1642.
Cornier-Quiquandon, M., Gratias, D. & Katz, A. (1991). In *Methods of Structural Analysis of Modulated Structures and Quasicrystals*, edited by J. M. Perez-Mato, F. J. Zuñiga & G. Madariaga, p. 313. Singapore: World Scientific.
Cornier-Quiquandon, M., Quivy, A., Lefebvre, S., Elkaim, D., Heger, G., Katz, A. & Gratias, D. (1991). *Phys. Rev. B*, **44**, 2071–2084.
Elcoro, L., Perez-Mato, J. M. & Madariaga, G. (1993). *J. Non-Cryst. Solids*, **153/154**, 155–159.
Elcoro, L., Perez-Mato, J. M. & Madariaga, G. (1994). *Acta Cryst.* A**50**, 182–193.
Elswijk, H. B., Hosson, J. Th. M. de, Van Smaalen, S. & Boer, J. L. de, (1988). *Phys. Rev. B*, **38**, 1681–1685.
Janot, C., Boissieu, M. de, Dubois, J. M. & Pannetier, J. (1989). *J. Phys. Condens. Matter*, **1**, 1029–1048.
Janssen, T. (1986). *Acta Cryst.* A**42**, 261–271.
Janssen, T. (1988). *Phys. Rep.* **168**, 55–113.
Koester, L. (1977). *Neutron Physics*. New York: Springer.
Nelder, J. A. & Mead, R. (1965). *Comput. J.* **7**, 308–313.
Steurer, W. (1990). *Z. Kristallogr.* **190**, 179–234.
Steurer, W. (1991). *J. Phys. Condens. Matter*, **3**, 3397–3410.
Steurer, W. & Kuo, K. H. (1990). *Acta Cryst.* B**46**, 703–712.
Van Smaalen, S. (1989). *Phys. Rev. B*, **39**, 5850–5856.
Van Smaalen, S., Boer, J. L. de & Shen, Y. (1991). *Phys. Rev. B*, **43**, 929–937.
Yamamoto, A. (1992). *Phys. Rev. B*, **45**, 5217–5227.
Yamamoto, A., Kato, K., Shibuya, T. & Takeuchi, S. (1990). *Phys. Rev. Lett.* **65**, 1603–1606.